EVALUATION AND VALIDATION OF MULTI-PHYSICS FE METHODS TO SIMULATE BIRD STRIKE ON A WING LEADING EDGE

M. Guida [1], F. Marulo [1], M. Meo [2], and M. Riccio [3]

[1] Dept. of Aerospace Engineering, University of Naples "Federico II", Naples, Italy
[2] Material Research Centre, Dept. of Mechanical Engineering, The University of Bath, Bath, UK
[3] Alenia Aeronautica, viale dell'Aeronautica, Pomigliano d'Arco, Naples, Italy
micguida@unina.it

ABSTRACT

As a consequence of the significant number of birdstrikes occurring every year, civil and military aircraft need to be designed to cater for such potential bird impacts on various structural components, such as engine, leading edge etc… Due to the extremely complex and costly experimental facilities needed to test bird-strike resistance of aircraft structures, it is fundamental to develop tools able to simulate material and structural behaviour of aircraft components during a strike and therefore to provide fast and reliable support to the design process. This paper reports a numerical campaign aimed at investigating the modelling of bird strike using 2 different bird formulations namely, Lagrangian and Arbitrary Lagrangian Eulerian (ALE) on a leading edge of a wing of a civil aircraft using the explicit finite element code MSC/Dytran [1]. In the Lagrangian formulation the finite element mesh follows the motion of the material, where each element represents the same piece of material through out the whole simulation and it is usually not suitable to simulate structures undergoing large deformations. Using this approach the bird was modelled using Lagrangian brick finite elements with the properties of a fluid, [1].
In an Arbitrary Lagrangian Eulerian (ALE) formulation the mesh is free to move independently to the material flow allowing the bird material to move through the mesh with consequent unlimited deformations. Using this approach, the bird flows through an Eulerian mesh to impact the structural finite element model. The Eulerian bird elements apply load to the structure elements through an ALE (Arbitrary Lagrange-Euler) coupling algorithm. This method does not need remeshing and is used for fluid dynamics simulations. The analyses were validated by performing experimental bird-strike tests on a sandwich wing leading edge from flexcore and aluminium alloys skins wing leading edge.

1 INTRODUCTION

Bird strikes happen most often during take off or landing, or during low altitude flight. However, bird strikes have also been reported at high altitudes, some as high as 6000 to 9000meters above ground level. According to the FAA, Federal Aviation Administration, wildlife hazard management manual for 2005, less than 8% of strikes occur above 900meters (3000feet) and 61% occur at less than 30meters (100feet). In general, the force of the impact on an aircraft depends on the weight of the animal and the speed difference and direction at the impact. The energy of the impact increases with the square of the speed difference. Hence a low-speed impact of a small bird on a car windshield causes relatively little damage. High speed impacts, as with jet aircraft, can cause considerable damage and even catastrophic failure to the vehicle. However, according to the FAA only 15% of strikes actually result in damage to the aircraft. The impact of a 5kg (12pound) bird at 240km/h (129kts) equals that of a 1/2 ton (1000pound) weight dropped from a height of 3meters (10feet).
The point of impact is usually any forward-facing edge of the vehicle such as a wing leading edge, nose cone, jet engine cowling or engine inlet. This paper describes the basic assumptions of the dynamic analysis about the bird strike crushing the leading edge. The idea is the result of the research project between the department of Aerospace

Structure at Naples University and Alenia Aeronautica. This project took aim to describe how the simulation can be carried out in an industrial environment to obtain the certification of a leading edge of a cargo airplanes, C27J, to a bird strike requirements. According to Federal Aviation Regulations section 23.631 “Bird Strike Damage” the leading edge of a wing must be defined in terms of structural resistance. In particular the requirements states that after the impact with an 8-pound bird at the impact speed equal to 135m/s (262kts), it is the cruise velocity Vc at sea level of the C27J, the leading edge should be not perforated and in case of high deformations no critical damage must be induced to the front spar sited behind the leading edge.
The leading edge of the fin structure of the C27J aircraft has a total length of 2970meters (117in), with a chord that varies between 450mm and 750mm (18in and 30in), see figure 1. The objective of this study was to verify the basic assumption of the analysis and to monitor the bird impact on fin structure in composite adopting the Lagrangian and Arbitrary Lagrange Euler (ALE) approach to investigate the validity of engineering impact resistance models for analysis of a bird strike. The numerical finite element simulations were performed using the commercial explicit integration code MSc Dytran. The experimental results are correlated to booth methods considering advantages and disadvantages of the different techniques of modelling.

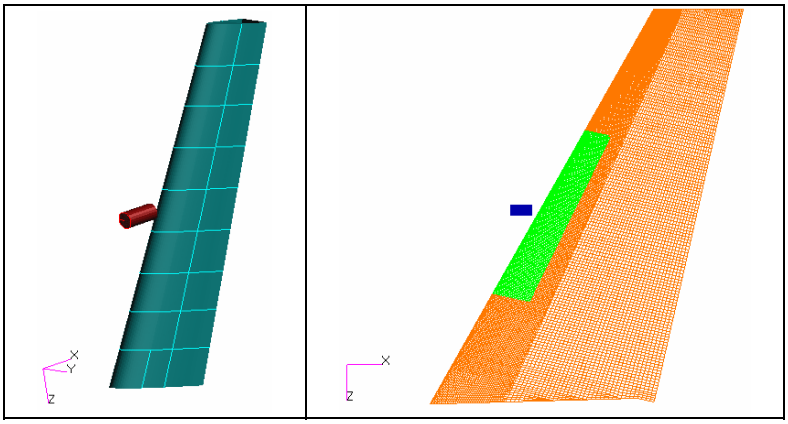

figure 1 – General view of the leading edge and its assembly on the fin of C27J

2 DESCRIPTION OF THE SURFACE

The layup of the leading edge was made three different plies, the outboard and inboard ply in aluminium alloy 2024T3, and the core in a honeycomb material. The outboard ply has a thickness of 1.4mm, the inboard ply has a thickness of 0.4mm. The sandwich structure has a thickness of 6.35mm, placed between two metallic face plates. This configuration was designed, built and subjected to bird strike tests.

3 EXPERIMENTAL SETUP

Tests are conducted using an air pressure gun, that is able to shoot dummy birds at the speed desired. The gun facility is sited at Alenia plant, see figure 2, it consists of a barrel length of 12m capable to speed up to 140m/s, with a pressure until 1.75MPa.
The projectile must be impacted onto leading edge at mid height just on the target, the position of the fin related to the water line of the airplane is shown in the figure 3, the sweepback angle of 63° reduces the load peak on the surface during the strike because the bird tends to slide on the leading edge.

figure 2 – Photos of the air pressure gun facility

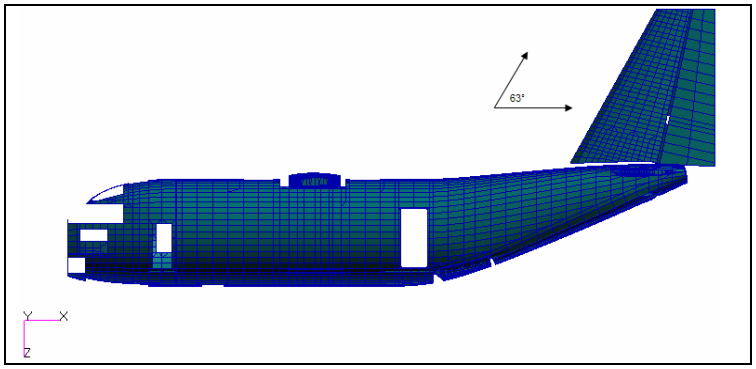

figure 3 – Fin position related to water line of the C27J aircraft

The velocity of the projectile is measured by two photocells mounted between the muzzle and the sabot separator. Two high-speed cameras were used to visualize the impact sequence. The support frame was suspended by means of six load cells, which measured loads transmitted to the foundations in three coordinate directions. The data acquisition system was a typical high speed system.

4 FINITE ELEMENT: MATERIAL PROPERTIES

This section refers to the material types used to model the distinct parts of the leading edge. A lot of different types of material models were used from the library of the MSC-DYTRAN code in the development of finite element analysis:
Dymat26 ‘‘Orthotropic Crushable Material Model
Dmatep “Isotropic Elastic–Plastic Model”

4.1 Honeycomb

The sandwich structure consists of a hexweb aluminium flexcore developed by Excel, the cells have been manufactured from aluminium alloy 5052 with height of 6.35mm. The honeycomb is placed between two metallic face plates. The significant mechanisms of energy absorption of these structures are the localized crushing of the core and the bending and stretching of the facings, while energy may be effectively absorbed through both local crushing and global deflection of the structural element as a whole. The core of a sandwich material must posses increased strength in shear to avoid relative sliding

of the face plates when a bending deformation is applied on the sandwich panel. For the honeycomb core material modelling, the "Orthotropic Crushable Material Model" was used, where the properties and the corresponding experimental stress–strain curve under edgewise compression, required as input parameters, are given in Table 1 and figure 4, respectively. The input required for the material consists of two parts: data for the fully compacted state and data for the crushing behaviour. For the fully compacted material, the input consists of the density, the elastic modulus for the fully compacted material, Poisson's ratio for the fully compacted material, the yield stress for the fully compacted material, and the relative volume at which the material is fully compacted. The behaviour during crushing is orthotropic and is characterized by uncoupled strain behaviour when the initial Poisson's ratios are not supplied. During crushing, the elastic modules vary from their initial values to the fully compacted values. This variation is linear with relative volume. When the material is fully compacted, the behaviour is elastic perfectly plastic with isotropic plasticity.

Young's modulus for the fully compacted material [GPa]	max shear Direction L τ_L [MPa]	Max shear Direction W τ_w [MPa]	G13 [MPa]	G23 [MPa]
0.9	0.8	1	90	220

Table 1 – Core Material Properties

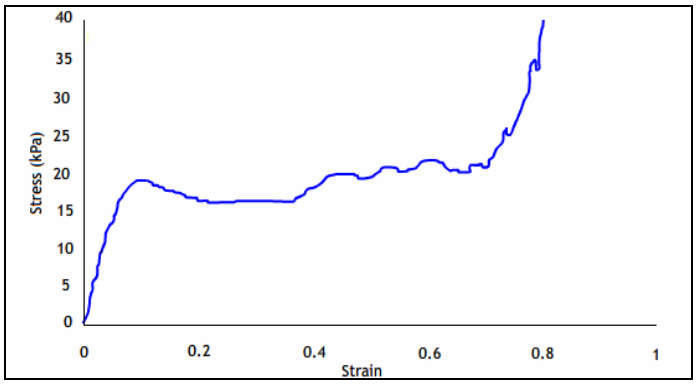

figure 4 – Experimental compression stress-strain curve

The stress-strain curve has three distinct regions: the first part of curve is characterized from predominant contribution to the elastic strain comes from the vertical compression. The elastic region is characterized by the effective Young modulus of the material, that is the Young modulus of an uniform material that for the same imposed stresses gives rise to the same strains. This is found by taking the slope of the unloading curve, which helps to reduce the effects of any local plastic flow. The second part of graph shows the aluminium honeycomb will start to plastically deform if the stress in the faces anywhere exceeds the flow stress, σ_Y, of the aluminium cell wall. The yielding behaviour started when the maximum stress in each face reaches the flow stress, σ_Y, of the material making up the cell walls, [2] that is given by:

$$\sigma = \frac{4}{9} \cdot \left(\frac{t}{l}\right)^2 \cdot \sigma_y \qquad \text{(eq. 1)}$$

Considering that *t* is thickness of an individual sheet and it is equal to 0.145mm, *l* is the length of each of the cell faces and it is equal to 6.35mm σ_y=100MPa, the yielding behaviour started when the stress is 34.7KPa.

4.2 Aluminium alloy 2024-T3

The material law used for the aluminium layers was an isotropic elastic–plastic thin shell model, where it has defined a bilinear yield model with isotropic hardening using von Mises yield criterion with a plasticity algorithm that includes the strain rate effects at medium regime using the Cooper Symonds law:

$$\frac{\sigma_n}{\sigma_y} = 1 + \left(\frac{\dot{\varepsilon}}{D}\right)^{1/p} \qquad \text{(eq. 2)}$$

where σ_n is the dynamic stress, σ_y is the elastic yield stress and dε/dt is the equivalent stress strain rate, whereas D=1.28E^5 and p=4 are constant in Cooper Symonds law [3]. The failure criterion about the aluminium is the maximum plastic strain and according to [4] it has been fixed the maximum strain for 2024-T3 as 18%, so this was implemented via the isotropic damage law within the code. The properties of the material are:

Young modulus E [GPa]	Yield Stress σy [MPa]	Ultimate Strength σr [MPa]	Failure Strain
72	76	185	0.18

Table 2 – Properties Aluminium Alloy Material Parameters

5 BIRD MODELING

The explicit FE codes adopted various finite element methods to model the impact phenomena: the Lagrangian approach, techniques based on Eulerian or Arbitrary Lagrangian Eulerian (ALE) approach, and recently solvers based on Smoothed Particle Hydrodynamics (SPH) method. A part from the different approach adopted, these models have the same characteristics: the same geometry and the same material. In particular, the bird was modelled as a projectile with the shape of a cylinder. In this work we adopted the Lagrangian and ALE method.

5.1 LAGRANGIAN

The Lagrangian method uses material coordinates, also known as Lagrangian Coordinates, as the reference; these coordinates are generally denoted as X. The nodes of the Lagrangian mesh are associated to particles in the material under examination; therefore, each node of the mesh follows an individual particle in motion, this can be observed in figure 5.

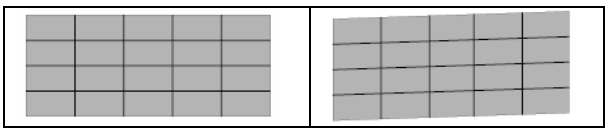

figure 5 – Lagrangian solver

The motion description for the Lagrangian formulation is:

$$x = \varphi(X, t) \quad \text{(eq. 3)}$$

where $\varphi(X, t)$ is the mapping between the current position and the initial position. The displacement u of a material point is defined as the difference between the current position and the initial position:

$$u(X, t) = \varphi(X, t) - X = x - X \quad \text{(eq. 4)}$$

The speed and acceleration are defined as the temporal derivates:

$$v = \frac{\partial}{\partial t}[x(X,t)] \qquad a = \frac{\partial^2}{\partial t^2}[x(X,t)] \quad \text{(eq. 5)}$$

At the end of the time step if current configuration is the same related to initial position it's considered a formulation is known as the Updated Lagrangian formulation, in this case the new reference is the current state. If the current configuration consists of a modified configuration then it possible consider the formulation is known as the Total Lagrangian formulation, which as reference considers the initial state, when t = 0. This formulation describes the motion because fixed the initial position it is possible to restore a kinetic history about any point. The imposition of boundary conditions is simplified since the boundary nodes remain on the material boundary. Another advantage of the Lagrangian method is the ability to easily track history dependant materials. However, a Lagrangian description of this problem may result in loss of bird mass due to the fluid behaviour of the bird which causes large distortions in the bird. In an explicit finite element analysis, the time step is determined by the smallest element dimension. The severe mesh distortion caused the time step to decrease to an unacceptably low value for the calculations to continue. These excessive distortions cause failure due to volumetric strain in some elements of the modelled bird. The problem is to determine the initial contact pressure during a strike, Wilbeck, [1], gave a comprehensive description of the impact of a soft cylindrical projectile against a rigid plate. When the soft projectile impacts the target, a shock wave is formed when particles on the front surface of the projectile are instantaneously brought to rest relative to the target. The pressure in the shock region is very high initially and is constant throughout the shock region. As the shock propagates, a complicated stress field with high pressure gradients develops in the projectile. If, at any time, the state of stress exceeds the strength of the material, the material "flows" like a fluid. After several reflections of the stress waves, a condition of steady flow is established. The initial contact pressure is called the Hugoniot pressure and it can be described as:

$$p = \rho_1 u_s u_0 \quad \text{(eq. 6)}$$

where ρ_1 is the density of the projectile, u_s is the shock wave velocity, and u_o is the projectile's initial velocity. In equation 6 the initial peak pressure depends only on densities and velocities and not on the length or cross-sectional area of the projectile. The weight of bird used in the impact testing was 3.6kg, the density was ρ=950kg/m^3 and pressure value considered is 1890MPa.

5.2 ALE

In the Eulerian solver, the grid points are fixed in space and the elements are simply partitions of the space defined by connected grid points. The Eulerian mesh is a "fixed frame of reference." The material of a body under analysis moves through the Eulerian mesh; the mass, momentum, and energy of the material are transported from element to

element. The Eulerian solver, therefore, calculates the motion of material through elements of constant volume, figure 6.

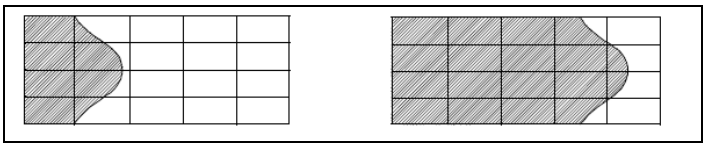

figure 6 – Eulerian solver

It is important to note that the Eulerian mesh is defined in exactly the same manner as a Lagrangian mesh. General connectivity is used so the Eulerian mesh can be of an arbitrary shape and have an arbitrary numbering system. This offers considerably more flexibility than the logical rectangular meshes used in other Eulerian codes. Using the Eulerian bird technique, the bird flows through an Eulerian mesh to impact the structural finite element model. The Eulerian bird elements apply load to the structure elements through an ALE (Arbitrary Lagrange-Euler) coupling algorithm. In both cases the structure model is constructed with Lagrangian finite elements. This method does not need remeshing and is used for fluid dynamics simulations. The major disadvantages of the method are that the resolution of flow definition and interface definition is less than in other approaches. In the ALE method, the reference is chosen arbitrarily to use the optimal method for each step of the simulation. For the ALE method, the simulation is split into a Lagrangian phase, an Eulerian phase and a smoothing phase in between. Because of this, greater distortions of the material can be handled than those allowed by the Lagrangian method with higher resolution and the Eulerian approach. The solution of Eulerian approach is based on a so-called Riemann solution at the element faces that defines the fluxes of mass, momentum and energy, the conserved problem quantities. The non viscous flow of a fluid is fully governed by the Euler equations of motion. We will use the equations in their conservative form:

$$\frac{\partial q}{\partial t}+\frac{\partial f(q)}{\partial x}+\frac{\partial g(q)}{\partial y}+\frac{\partial h(q)}{\partial z}=0 \qquad \text{(eq. 7)}$$

where q is the state vector and $f(q)$, $g(q)$ and $h(q)$ represent the fluxes of the conserved state variables. They are defined as follows:

$$q=\begin{pmatrix}\rho\\ \rho u\\ \rho v\\ \rho w\\ E\end{pmatrix} \quad f(q)=\begin{pmatrix}\rho u\\ \rho u^2+p\\ \rho uv\\ \rho uw\\ (E+p)u\end{pmatrix} \quad g(q)=\begin{pmatrix}\rho v\\ \rho uv\\ \rho v^2+p\\ \rho vw\\ (E+p)w\end{pmatrix} \quad h(q)=\begin{pmatrix}\rho w\\ \rho uw\\ \rho vw\\ \rho w^2+p\\ (E+p)w\end{pmatrix} \qquad \text{(eq. 8)}$$

The equations describe the conservation of mass, momentum and energy. In Eq.8, ρ is the material density, u, v, and w are the velocity components, p is the pressure and E the total energy. For a fluid in its simplest form, we many use a so-called “simple bulk” equation of state:

$$p=k\left(\frac{\rho}{\rho_0}-1\right) \qquad \text{(eq. 9)}$$

In eq.10 K is the material bulk modulus and ρ_0 is the reference density at which the material has no pressure. Also which the material has no pressure. The conservation laws are numerically solved by an upwind, cell-centered finite volume method on

unstructured 3-D meshes. The Eulerian solver calculates the motion of material through elements of constant volume.

6 RESULTS

The finite element analysis is performed on the fin, the figure 7 shows the stress distribution on the structure adopting the Lagrangian approach:

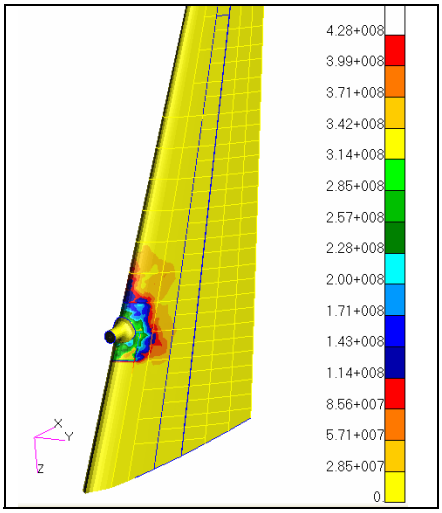

figure 7 – contour of max stress on the C27J fin finite model – Lagrangian approach

The figure 7 shows the impact sequence in one of the scenarios analysed for the leading edge, this picture shows that the damage produced to the structure is local, only small portion of the leading edge is damaged by the strike, whereas the rest of structure remains in the elastic range. The fringe plot shows the stress distribution in the KPa, that values underline the peak stress of 400MPa is located in the contact zone. The simulations show that the leading edge is able to withstand the specified impact without the bird penetrating in the structure.

Whereas the ALE approach underline the fluid behaviour of the bird. The figure 8 shows the sequence of the impact on the fin. From images it is possible see the cylinder movement that were lapping on the structure deforming the fin during the transfer of the kinetic energy. This damage is far less severe than the damage caused adopting a Lagrangian approach.

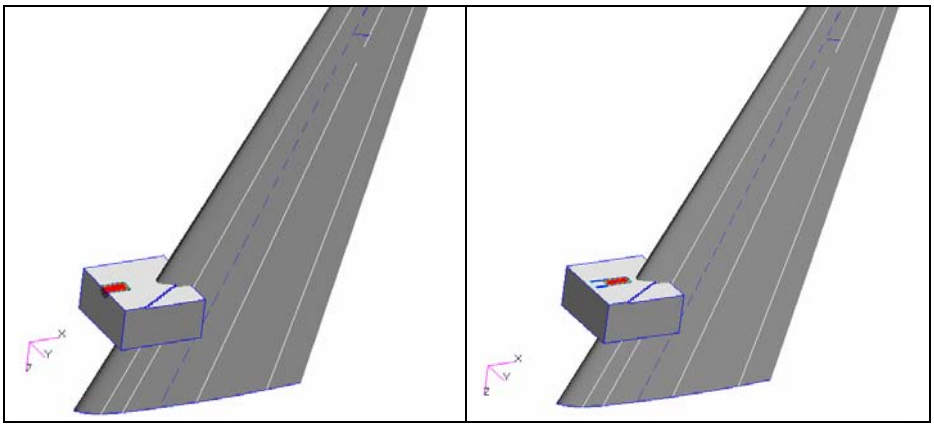

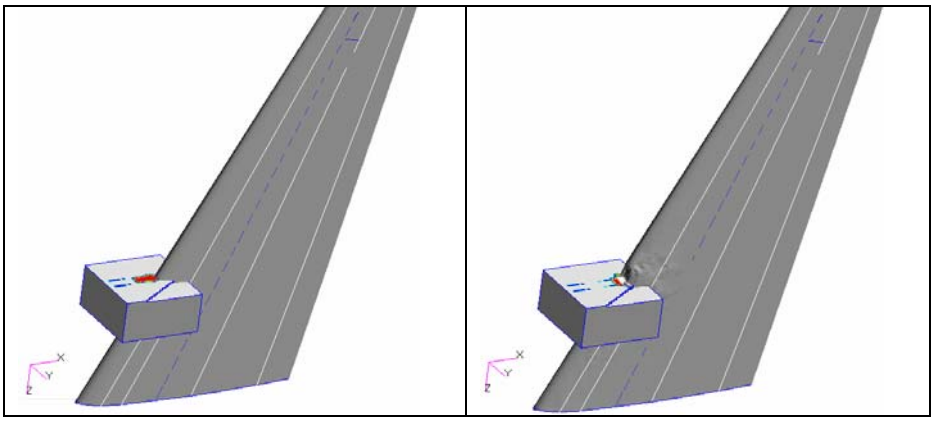

figure 8 – C27J fin finite model – ALE approach

The possibility to consider the bird like a hydrodynamic phenomenon, ALE approach, costs disadvantages about the computational runtime related to Lagrangian approach.

	LAGRANGIAN APPRACH	ALE APPROACH
ELEMENTS #	133.163	133.163
RUNTIME	2hours and 40minuts	22hours

Table 3 – Comparison between runtime about Lagrangian and ALE Approach

The other disadvantage it is the peak of contact force, in the figure 9 ALE approach undervalues the real contact. According to the experimental value recorded by load cell the contact force is 4000daN, this value is been correlate by Lagrangian approach, but the ALE approach is lower.

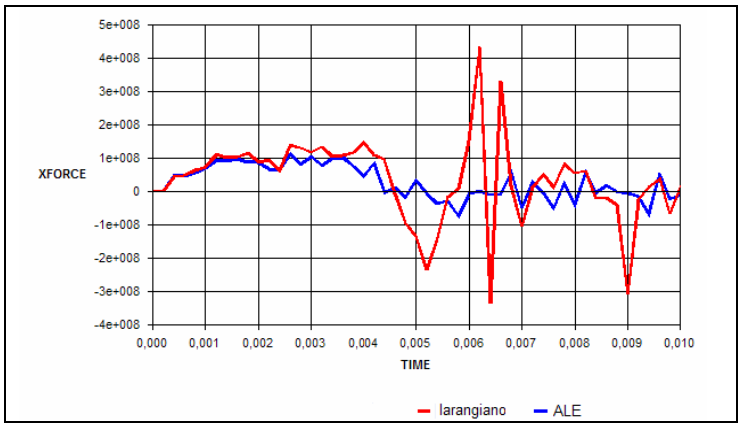

figure 9 – Contact force time history by Lagrangian and ALE approach

The typical response of a composite leading edge is plotted in figure 10. The out of plane displacement is measured in the centre of the plate. The experimental deformation of the leading edge is 120mm, this value is equal to the Lagrangian approach, whereas the deformations results underestimate according to ALE approach.

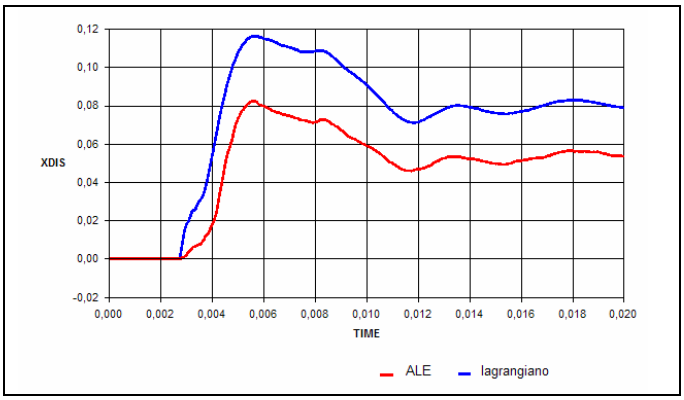

figure 10 – THS della deformata massima con tecnica lagrangiano e ALE

7 CONCLUSIONS

This paper presents the preliminary results of a collaborative project between academic and industrial partners to evaluate the impact properties of composite material with layers of aluminium alloy used for aircraft parts likely to be subjected to bird strikes. The study was driven by the industrial demand to improve the design rules necessary for the preliminary evaluation of the structural response of a leading edge of a new aircraft, when subject to bird strike. A detailed finite element model was built using the commercial explicit integration code MSc/Dytran. The simulations included the leading edge and the structure supporting the test article using two different bird formulations: Lagrangian and ALE. The final correlation between numerical and experimental showed that good correlation was achieved, in terms of global structural behaviour of the test article, confirming the validity of the Lagrangian approach. In particular, the ALE approach defined a difficulty in the model and in the post processing phase, then this approach has been defined with a heavy runtime, moreover the peak of the impact force and the maximum deformation has been underestimate by the ALE approach, whereas the using the Lagrangian approach the model was accurate to predict the final deformed shape of the leading edge and the absence of foreign object penetration, showing that the designed leading edge made with honeycomb and aluminum material was able to protect the inner Leading edge structure from damaging and to satisfy certification requirements.

8 REFERENCES

1. MSC/Dytran Reference Manual.
2. Wilbeck, J. S., “Impact Behaviour of Low Strength Projectiles,” *Ph’D. Dissertation, Texas A&M Univ., College Station, TX, 1977.*
3. Scott D. Papka And Stelios Kyriakides. “In-Plane Compressive Response And Crushing Of Honeycomb”, *Mech. PhJs. Solids,Vol. 42, No. 10, pp. 1499-1532, 1994 Elsevier Science Ltd.*
4. A. Airoldi, B. Cacchione, “Numerical Analysis of bird impact on aircraft structures undergoing large deformations and localised failure”, *WIT Transactions on Engineering Sciences, Vol 49, Impact Loading of Lightweight Structures, M. Alves & N. Jones (Editors), 2005.*
5. M.A.Mccarthy, J.R.Xiao, N.Petrinic, A.Kamoulakos And V. Melito, “Modeling of Bird Strike on an Aircraft Wing Leading Edge Made from Fibre Metal Laminates” – Part 1: Material Modeling, *Applied Composite Materials 11: 295–315, 2004.*